there must be a critical value of throat radius r_t such that for $r_t < r_t$ the effective nozzle area actually decreases with decreasing r_t because of the rapid boundary-layer growth This conclusion follows from the expression

$$(A_{eff}/A_t) = (R - \delta_1)^2/r_t^2 = R^2[(1/r_t) - A/(r_t^{2\gamma\lambda} + 1)]^2 \quad (8)$$

which has a maximum value when

$$r_t = r_t = [(2\gamma\lambda + 1)K]^{1/2\gamma\lambda} \quad (9)$$

For example, for the nozzle considered previously when $p_0 =$ 4000 atm, $h_0/RT_R = 220$, $r_{tc} = 0\ 0123$ in , and when $p_0 =$ 200 atm, $h_0/RT_R = 180$, $r_t = 0\ 0342$ in At low stagnation pressures the critical throat radius is thus rather close to the actual values used

References

[1] Johnson, R H , "Hypersonic viscous effects in wind tunnels," ARS J **31**, 1022–1024 (1961)

[2] Burke, A F and Bird, K D , "The use of conical and contoured expansion nozzles in hypervelocity facilities," *Advances in Hypervelocity Techniques* (Plenum Press, New York, 1962), pp 373–424

[3] Hayes, W D and Probstein, R F , *Hypersonic Flow Theory* (Academic Press, New York, 1959), pp 296–298

[4] Reece, J W , "Test section conditions generated in the supersonic expansion of real air," J Aerospace Sci **29**, 617–618 (1962)

[5] Sichel, M , "The effect of the boundary layer upon the flow in a conical hypersonic wind tunnel nozzle," Dept Aeronaut Astronaut Eng , Univ Michigan, Rept 02953-2-F (July 1963)

[6] Feldman, S , 'Hypersonic gas dynamic charts for equilibrium air, ' Avco Res Lab , Res Rept 40 (January 1957)

[7] Goin, K L , "Mach tables for real gas equilibrium flow of air in hypervelocity test facilities with total temperatures to 10,000°K," Sandia Corp , Rept SCR 288 (March 1961)

[8] Blackwell, F , "Properties of argon free air, 'Ramo-Wooldridge Corp , Los Angeles, Calif , Rept GM-TR-76 (October 1956)

[9] Lukasiewicz, J , "An assessment of our present status and further requirements for high temperature hypersonic facilities, round table discussion," Training Center for Exptl Aerodynamics, Rhode Saint Genese, Belgium, TCEA TM 14 (April 6, 1962)

Intermolecular-Force Effects on the Thermodynamic Properties of Nitrogen

C Edward Smith Jr *

Lockheed Missiles and Space Company, Palo Alto, Calif

Nomenclature

B = second virial coefficient, cm³/mole
C = third virial coefficient, (cm³/mole)²
D = fourth virial coefficient, (cm³/mole)³
e = internal energy, cal/mole
h = enthalpy, cal/mole
p = pressure, atm
R = gas constant, 1 9872 cal/mole K
s = entropy, cal/mole-°K
T = temperature, °K
Z = compressibility factor
ρ = density, mole/cm³
ρ_0 = reference (or normal) density, 4 4634 × 10^{-5} mole/cm³

Received October 29, 1963 This work was performed as a part of the Lockheed Missiles and Space Company Independent Research Program

* Associate Research Scientist, Physical Sciences Laboratory Member AIAA

Introduction

A KNOWLEDGE of the thermodynamic properties of the working gas is essential to the analysis of data measured in wind tunnels The present emphasis on high stagnation temperatures, coupled with the widespread usage of nitrogen in hot-shot and shock tunnels, has brought about a comprehensive documentation of the properties of nitrogen [1–6] Reference 6, in fact, presents calculations of properties up to 100,000°K and includes ionized species up to N^{5+}! Neglected in most of these calculations at high temperatures are the equally important high-density effects on thermodynamic properties caused by the intermolecular (or so-called van der Waals) forces

Although Hilsenrath et al [1] included intermolecular-force effects, their tables extend to only 100 times normal pressure The corresponding density ratio is less than 25 for tempera tures greater than 1000°K, and the intermolecular-force effects are small Grabau et al [7] computed values for much higher densities (up to 300 times normal) but only for the limited temperature range of 3000° to 4000°K

This paper presents increments in the thermodynamic state variables of nitrogen (based on the virial coefficients of Amdur and Mason[8]) caused by intermolecular forces These increments in dimensionless form, $\Delta e/RT$, $\Delta s/R$, and Z, are plotted as functions of temperature and logarithm of density ratio The present results are presented for densities up to 300 times normal at temperatures between 1000° and 9000°K However, because of dissociation, the accuracy probably is not good above 6000°K

Method

The thermodynamic effects of the intermolecular forces can be included if we express the virial equation of state in powers of density as

$$p = \rho RT(1 + \rho B + \rho^2 C + \rho^3 D) = \rho RTZ \quad (1)$$

where B, C, and D are virial coefficients and are functions only of temperature Reference 9 contains equations for the increments in internal energy, enthalpy, and entropy caused by the intermolecular forces In terms of the virial coefficients, they are

$$\frac{\Delta e}{RT} = -\left[\rho T\frac{dB}{dT} + \frac{\rho^2}{2}T\frac{dC}{dT} + \frac{\rho^3}{3}T\frac{dD}{dT}\right] \quad (2)$$

$$\frac{\Delta h}{RT} = \frac{\Delta e}{RT} + (Z - 1) \quad (3)$$

and

$$\frac{\Delta s}{R} = -\left\{\rho T\frac{dB}{dT} + \frac{\rho^2}{2}\left[B^2 - C + T\frac{dC}{dT}\right] - \frac{\rho^3}{3}\left[B^3 - 3BC + 2D + T\frac{dD}{dT}\right]\right\} \quad (4)$$

The virial coefficients, B, C, and D, for nitrogen, tabulated by Amdur and Mason[8] for the temperature range of 1000° to 15,000°K, were used in the present calculations Since derivatives of the coefficients with respect to temperature are needed in Eqs (2) and (4), a polynomial representation of each coefficient was computed to facilitate differentiation A seventh-degree polynomial was fitted by means of the method of least squares through the 24 points for each virial coefficient In this manner, each coefficient was represented by an equation of the form

$$X(T) = x_0 + x_1T + x_2T^2 + \quad + x_7T^7 \quad (5)$$

where T is in degrees Kelvin The curve fitting was done with a digital computer The polynomial coefficients that were calculated are contained in Table 1 It should be noted that the polynomials fit the values of B, C, and D over the entire

Table 1 Coefficients of polynomials used to represent virial coefficients

Term no	$B(T)$, cm³/mole	$C(T)$, (cm³/mole)²	$D(T)$, (cm³/mole)³
0	22 517659	1 5279260 × 10^{3}	5 0670219 × 10^{4}
1	1 0321382 × 10^{-2}	−0 72037852	−34 331275
2	−4 1612639 × 10^{-6}	2 3150284 × 10^{-4}	1 2896822 × 10^{-2}
3	8 5980195 × 10^{-10}	−4 4333676 × 10^{-8}	−2 7784221 × 10^{-6}
4	−1 0654868 × 10^{13}	5 0471715 × 10^{-12}	3 5171097 × 10^{-10}
5	7 7697577 × 10^{18}	−3 3492819 × 10^{-16}	−2 5786019 × 10^{-14}
6	−3 0447773 × 10^{22}	1 1955060 × 10^{-20}	1 0110035 × 10^{-18}
7	4 9238351 × 10^{-27}	−1 7731931 × 10^{-25}	−1 6372610 × 10^{-23}

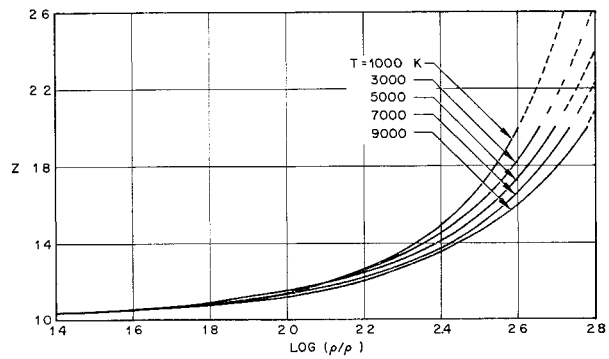

Fig 1 Compressibility factor

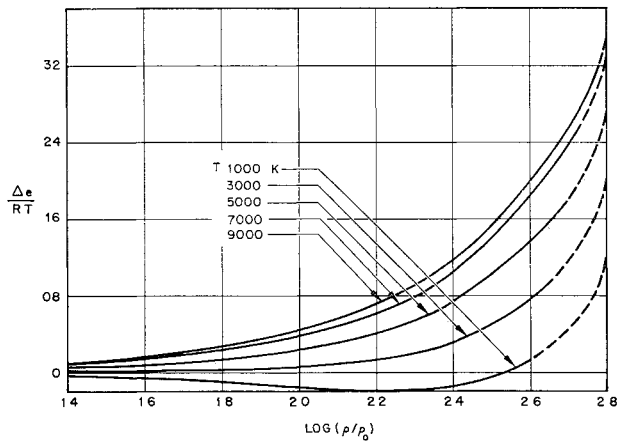

Fig 2 Internal energy increment

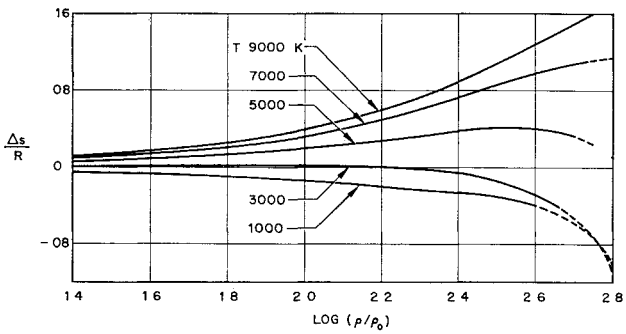

Fig 3 Entropy increment

temperature range, although the calculations contained in this paper extend up to only 9000°K

Results

Figure 1 contains the compressibility factor, Fig 2 the internal energy increment, and Fig 3 the entropy increment as functions of logarithm of density ratio, with temperature as a parameter Results corresponding to values of Z greater than 2 0 are shown dotted, since more than four terms of the virial equation probably should be taken at the higher densities to assure adequate accuracy In practice, however, the higher coefficients of the virial equation are known with less certainty, and the improvement gained by including them is somewhat doubtful Enthalpy increment can easily be obtained by means of Eq (3) It can be seen from Figs 1–3 that the corrections to the thermodynamic properties due to the intermolecular-force effects are small for densities less than 25 times normal For greater densities, the corrections are appreciable and probably should be included for most applications It should be noted that intermolecular-force effects were not included in the Mollier diagram presented in Ref 4, although densities as high as 1000 times normal are plotted A more accurate description of the properties of nitrogen can be obtained by adding the increments contained herein to the values in Ref 4 and replotting the Mollier diagram for the higher values of density

Thermodynamic properties were calculated by adding the increments due to intermolecular-force effects to a simple kinetic-theory description of nitrogen as an ideal diatomic gas The results of this calculation are presented in Ref 10 The values of the state variables thus obtained were compared with the data contained in Refs 1–3 and 7 Throughout most of the range, the agreement was very good, and the differences were less than 1% The only serious disagreement is in the region where the effect of molecular dissociation is significant The effects of dissociation were not included in Ref 10 Since the virial coefficients were derived for collisions between nitrogen molecules only, the increments in thermodynamic properties are not accurate when significant dissociation exists

References

[1] Hilsenrath, J , Beckett, C W , Benedict, W S , Fano, L , Hoge, H J , Masi, J F , Nuttall, R L , Touloukian, Y S , and Wooley, H W , *Tables of Thermodynamic and Transport Properties* (Pergamon Press, London, 1960), pp 237–368

[2] Treanor, C E and Logan, J G , "Thermodynamic properties of nitrogen from 2000 K to 8000°K," BE-1007-A-5, Cornell Aeronaut Lab , Buffalo, N Y (January 1957)

[3] Little, W J and Neel, C A "Tables of the thermodynamic properties of nitrogen from 100 to 1500°K," AEDC-TDR-62-170, Arnold Eng Dev Center, Arnold Air Force Base, Tenn (September 1962)

[4] Humphrey, R L , Little, W J , and Seeley, L A , "Mollier diagram for nitrogen," AEDC-TN-60-83, Arnold Eng Dev Center, Arnold Air Force Base, Tenn (May 1960)

[5] Buckingham, A C , "Thermodynamic properties of high-temperature nitrogen," 6-90 62-124, Lockheed Missiles and Space Co , Sunnyvale, Calif (December 1962)

[6] Sewell, K G and Fenter, F W , "The thermodynamic properties of high-temperature nitrogen," 0-71000/2R-25, Ling Temco Vought, Dallas, Texas (July 1962)

[7] Grabau, M , Humphrey, R L , and Little, W J , ' Determination of test section, after-shock, and stagnation conditions in hotshot tunnels using real nitrogen at temperatures from 3000 to 4000°K," AEDC-TN-61-82, Arnold Eng Dev Center, Arnold Air Force Base, Tenn (July 1961)

[8] Amdur, I and Mason, E A , "Properties of gases at very high temperatures," Phys Fluids 1, 370–383 (1958)

[9] Hirschfelder, J O , Curtiss, C F , and Bird, R B , *Molecular*

Theory of Gases and Liquids (John Wiley and Sons Inc , New York, 1954), pp 230–232

[10] Smith, C E , "Thermodynamic properties of nitrogen," 6-90-62-111, Lockheed Missiles and Space Co , Sunnyvale, Calif (December 1962)

Supersonic Stagnation Point Heat Transfer at Low Reynolds Numbers

HENRY TONG*
Boeing Company, Seattle, Wash

and

W H GIEDT†
University of California, Berkeley, Calif

Stagnation point heat transfer at low Reynolds numbers in a supersonic air stream was investigated experimentally A transient technique was employed using precooled thin-walled hemisphere-cylinder models Results were obtained for nominal Mach numbers of 2, 4, and 6 and in the Reynolds number (based on conditions behind the bow shock and model diameter) range of 80 to 1500 These results are in good agreement with continuum boundary-layer theory down to a Reynolds number of approximately 300 At values below this an increase approaching 10% is indicated

Nomenclature

c_p = specific heat at constant pressure
d = cylinder and hemisphere diameter
h = heat-transfer coefficient = $q/(T_0 - T_w)$
k = thermal conductivity
M = Mach number
Nu = Nusselt number = hd/k
Pr = Prandtl number = uc_p/k
q = stagnation point heat rate
Re = Reynolds number = $\rho Ud/\mu$
T = absolute temperature
$\tilde{u}'$ = $[d(U/U_2)/d(x/d)]$
U = velocity
x = distance from stagnation point
ϵ = density ratio across normal shock
μ = viscosity
ρ = density

Subscripts

0 = stagnation reservoir
1 = upstream of shock
2 = downstream of shock
BL = boundary-layer value
e = edge of boundary layer

I Introduction

REPRESENTATIVE results of recent studies of the heat transfer to the stagnation point of a blunt body at low Reynolds numbers are summarized in Fig 1 Analytical investigations have considered various second-order effects ordinarily neglected in classical boundary-layer theory These include vorticity introduced as the flow passes through the bow shock wave, slip, and temperature jump ‡ To indicate the importance of these second order effects, comparisons are made with continuum boundary-layer results[2] extrapolated to low Reynolds numbers

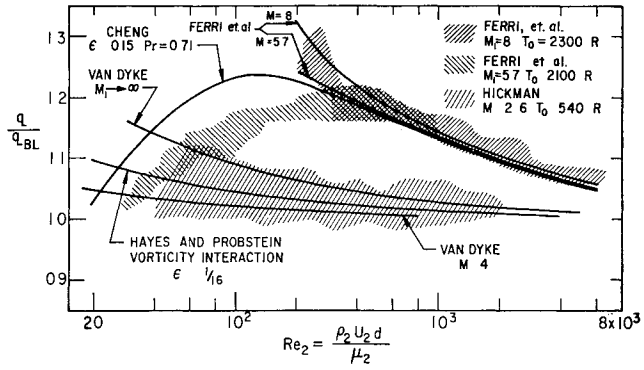

Fig 1 Comparison of theoretical and experimental stagnation point heat transfer

Two trends are apparent in Fig 1 The first is supported by the theories of Ferri, Zakkay, and Ting,[3] Cheng,[4] and the data of Ferri et al [3 5] This shows an increase in heat transfer above continuum boundary-layer values starting at Re_2 of about 20,000 and increasing to a maximum of 25% at $Re_2 \sim 150$ The second trend[1 6–8] indicates the heat transfer begins to rise above the continuum boundary-layer value at magnitudes of $Re_2 \lesssim 1000$ and that the increase is only about one-third to one-half that of the other results

No satisfactory explanation has been advanced for the differences in these two trends It was recognized, however, that the experimental data available were obtained in different test facilities and with different techniques Because of this it was decided that additional tests in the low-pressure wind tunnel at the University of California using a transient technique would be desirable Results obtained are presented herein

II Experimental Equipment and Procedure

Heat-transfer models were thin-walled hemisphere cylinders of electroplated nickel Three sizes were used: 0 250 in , 0 500 in , and 1 00 in in diameter, with 0 004 in nominal wall thicknesses Transient temperatures were measured by means of No 40 gage copper-constantan thermocouples welded into holes drilled at the stagnation points

The models were cooled below the wind tunnel stagnation temperature (~530°R) by enclosing them in a coil of copper tubing through which liquid nitrogen was pumped The coil was then suddenly removed and the model rotated rapidly into the tunnel air stream Further details of the construction techniques, instrumentation, and evaluation of the test results are given in Ref 9

III Results

The stagnation-point heat-transfer results determined are shown graphically in Fig. 2 in terms of the Nusselt number divided by the square root of the dimensionless velocity gradient at the edge of the boundary layer, $Nu/\tilde{u}_e'^{1/2}$, as a function of the Reynolds number downstream of the shock, Re_2 Evaluation of all temperature records yielded duplicate results for each test condition Since the variation of $Nu/\tilde{u}'^{1/2}$ obtained at any value of Re_2 was indicative of the experimental accuracy, all data points were included in Fig 2 As can be noted, only a few points fell outside the lines deviating ±10% from the continuum boundary-layer reference line

An average $Nu/\tilde{u}'^{1/2}$ was computed at each value of Re_2 for which two or more experimental points were available

Received November 8, 1963 Based on research supported by the Aeronautical Research Laboratory of the U S Air Force Aeronautical Systems Division under Contract No AF33(657)-8607

* Research Engineer, Aero-Space Division
† Professor of Aeronautical Sciences Member AIAA

‡ The various effects considered by different investigators are reviewed and discussed in Ref 1